

Bound states and resonance states of the plasma-embedded $pp\mu$ molecular ion

Sabyasachi Kar and Y. K. Ho

Institute of Atomic and Molecular Sciences, Academia Sinica, P.O. Box 23-166, Taipei, Taiwan 106, Republic of China

(Received 23 March 2007; published 19 June 2007)

We have investigated the effect of weakly coupled hot plasmas on the bound states and resonance states of the $pp\mu$ molecular ion. The plasma effect is taken care of by employing a screened Coulomb (Yukawa-type) potential, and highly correlated wave functions are used. The $^1S^e$ and $^3P^o$ resonances of the $pp\mu$ molecular ion in plasmas for different screening parameters below the $p\mu(2S)$ threshold are calculated using the stabilization method. The bound $^1S^e$ and $^3P^o$ state energies of the $pp\mu$ molecular ion are determined using a variational method. The $p\mu(1S)$ and $p\mu(2S)$ threshold energies for various screening parameters are also reported here.

DOI: [10.1103/PhysRevA.75.062509](https://doi.org/10.1103/PhysRevA.75.062509)

PACS number(s): 36.10.Dr, 52.20.-j, 32.70.Cs, 52.20.Hv

I. INTRODUCTION

The recent spectroscopy experiments on exotic atoms such as the $p\mu$ atom have established evidence on the existence of the $p\mu(1S)$ and $p\mu(2S)$ states [1–3]. The muonic hydrogen atoms are formed in highly excited states by sending the muons in a dense hydrogen target and the atoms rapidly decay to the ground $1S$ state or the metastable $2S$ states by several competing processes. With such processes, the $pp\mu$ molecule formation may take place in resonant collisions between the $p\mu(2S)$ state and the ordinary hydrogen molecules. In the PSI experiment [1,2], the kinetic energy distribution of the $p\mu(1S)$ atoms in a hydrogen gas was measured and a high-energy component in the vicinity of 900 eV was detected. It was interpreted in the observation of the high-energy component that the long-lived $p\mu(2S)$ state has probably been detected in a nonradiative quenching mechanism that involves the $pp\mu$ resonances below the $2S$ dissociation limit [1,2,4]. The Coulomb decay of those resonances lying in the vicinity of the 1800 eV above the $1S$ dissociation threshold may produce the $p\mu(1S)$ atoms. Recently, Coulombic and radiative decay rates of the exotic molecular ion $pp\mu$ have been calculated by Hilico *et al.* [5], by Lindroth *et al.* [6], and by Kilic *et al.* [7]. The bound states of the $pp\mu$ molecular ion have also been calculated using highly accurate correlated wave functions [8,9]. With the recent experimental developments on the $p\mu$ atoms [1–3], and with the recent theoretical progresses on various properties of the $pp\mu$ molecular ion [4–9], it is of great interest to investigate the effect of external environments like that of plasmas on the bound states and resonance states of the $pp\mu$ molecular ion.

Several theoretical investigations have been performed in recent years on two-electron atoms/ions immersed in Debye plasmas ([10–15] and references therein). Very recently, the stability of hydrogen molecular ion has also been investigated in plasma environments [16–19]. The importance of the Debye screening in atomic and molecular processes has been highlighted in the literature ([10–24], references therein). In the present work, we have carried out a theoretical investigation on the hot-plasma effects for the bound states and resonance states of the $pp\mu$ molecular ion in low rotational and vibrational levels using highly correlated wave functions. The Debye model has been used to simulate the

plasma effect, and the stabilization method [25–27] is used to extract resonance parameters. In the Debye concept of plasma modeling the interaction between two localized charge particles a and b can be represented by $Z \exp(-r_a - r_b/D)/|r_a - r_b|$, where $Z = q_a q_b$, q_a and q_b being the charges of the respective particles; the screening parameter D is called the Debye length. The stabilization method is a simple and powerful technique that needs only bound-state type basis functions to extract resonance energies and widths. In recent investigations it has been shown that the resonances obtained by using the stabilization method compared well with those obtained by using the complex-rotation method [15]. In this work, we concentrate ourselves on the $^1S^e$ and $^3P^o$ bound and resonance states of the $pp\mu$ molecular ion embedded in Debye plasmas.

II. CALCULATIONS

The nonrelativistic Hamiltonian describing the $pp\mu$ molecular ion immersed in Debye plasmas is given by

$$H = -\frac{1}{2m_p}[\nabla_1^2 + \nabla_2^2] - \frac{1}{2m_\mu}\nabla_3^2 - \left[\frac{\exp(-r_{31}/D)}{r_{31}} + \frac{\exp(-r_{32}/D)}{r_{32}} \right] + \frac{\exp(-r_{21}/D)}{r_{21}}, \quad (1)$$

where 1, 2, and 3 denote the two protons and the muon, respectively, $r_{ij} = |\vec{r}_i - \vec{r}_j| = r_{ji}$, and m_p and m_μ denote the masses of proton and muon, respectively. In this work, it is convenient to use the so-called quasiatomic unit [$\hbar = 1$, $e = 1$, $m_{\min} = 1$, and $m_{\min} = \min(m_p, m_\mu)$] [8]. To use the muon atomic unit ($\hbar = 1$, $e = 1$, $m_\mu = 1$), it is simplest to use $m_p = m = m_p/m_\mu$. The particle masses used in our present calculations are $m_p = 1836.152\,701\,m_e$, $m_\mu = 206.768\,262\,m_e$, with m_e denoting the electron mass. Throughout the work we have considered the muon atomic unit (m.a.u.) with $m = m_p/m_\mu = 8.88024440133854$. In the case of the muonic atoms, Bohr radius is roughly 186 times smaller than the ordinary atoms. The Debye length can be represented as $D = 1/\lambda = [k_B T / 4\pi n Z^2]^{1/2}$, n denotes the plasma density, T its temperature, and λ is the Debye screening parameters [23,24]. A set of plasma conditions can be simulated for different choices of D [m.a.u. (muon atomic unit)] as it depends on the

plasma density and plasma temperature. Here we briefly discuss the relationship between the muon a.u. and the conventional a.u. (emphasized in here as electron a.u.). The muon density n_μ takes the form as $n_\mu = 1.97 \times 10^{22} E_D/D^2 \text{ cm}^{-3}$ for $E_D = k_B T = 100 \text{ eV}$ and $Z=1$. The muon density is approximately equal to $2.2 \times 10^{21} \text{ cm}^{-3}$ when $D=30$ (electron a.u.), whereas the muon density is $n_\mu = 2.24 \times 10^{15} E_D/D^2 \text{ cm}^{-3} = 2.5 \times 10^{14} \text{ cm}^{-3}$ when $D=30$ m.a.u. It indicates that the muon density in $D=30$ m.a.u. is much lower than that in $D=30$ (electron a.u.). Our proposed model is hence more applicable in low-density and high-temperature plasmas. Details of such demonstration for two component plasmas near thermodynamic equilibrium can be well understood from the earlier reports [18,19,22,23].

For S and P states of the $pp\mu$ molecular ion, we use the following wave functions:

$$\Psi = (1 + S_{pn} \hat{O}_{21}) \sum_{i=1}^N C_i r_{31}^L P_L(\cos \theta_1) \exp[-\alpha_i r_{31} - \beta_i r_{32} - \gamma_i r_{21}] \omega, \quad (2)$$

where $\alpha_i, \beta_i, \gamma_i$ are the nonlinear variation parameters, C_i ($i=1, \dots, N$) are the linear expansion coefficients, $L=0$ for S states and $L=1$ for P states, $S_{pn}=1$ denotes the singlet spin states and $S_{pn}=-1$ indicates triplet spin states, N is the number basis terms, θ_1 is the angle between the \vec{r}_{31} and the unit vector along z axis [28], and P_L denotes the Legendre polynomial of order L . The operator \hat{O}_{21} is the permutation of the two-identical particles. The nonlinear variational parameters α_i, β_i , and γ_i are chosen from a quasirandom process ([8,9,13,14,21,28] and reference therein). In Eq. (2), ω is set equal to 1 for bound states calculations and it is varied for resonance calculations. The nonlinear parameters α_i, β_i , and γ_i are chosen from the three positive intervals $[A_1, A_2]$, $[B_1, B_2]$, and $[C_1, C_2]$:

$$\begin{aligned} \alpha_i &= \langle\langle i(i+1)\sqrt{2}/2 \rangle\rangle (A_2 - A_1) + A_1, \\ \beta_i &= \langle\langle i(i+1)\sqrt{3}/2 \rangle\rangle (B_2 - B_1) + B_1, \\ \gamma_i &= \langle\langle i(i+1)\sqrt{5}/2 \rangle\rangle (C_2 - C_1) + C_1, \end{aligned} \quad (3)$$

where the symbol $\langle\langle \dots \rangle\rangle$ designates the fractional part of a real number. The wave function (2) supported by the quasirandom (3) was widely used in several earlier works [8,9,13,14,21,28] and further references therein. As the wave function in Eq. (2) contains only exponential terms involving interparticle coordinates, the purely random process will yield numerically nearly linearly dependent matrix elements after few terms. So this Hylleraas-type exponential basis function (2) based on the nonlinear parameters chosen from the quasirandom process of the type (3) produce results with the same accuracy as obtained by any other type of Hylleraas basis [8].

III. BOUND STATES OF $pp\mu$ EMBEDDED IN DEBYE PLASMAS

To designate molecular states it is convenient to use the rotational (J) and vibrational (ν) quantum numbers. The

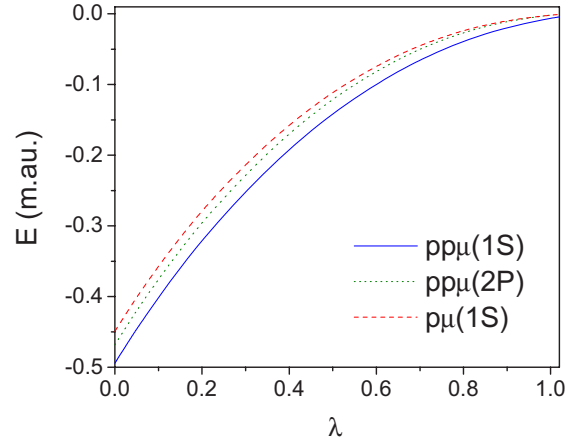


FIG. 1. (Color online) Bound states of the $pp\mu$ molecular ion under Debye screening.

three-body states can also be classified as gerade or ungerade depending on the combined effect of the spin (S) and parity (π), $\pi(-1)^S$, with the resulting plus sign denoting gerade and minus sign denoting ungerade. The atomic labels for the $J=0$ and $J=1$ gerade states are $^1S^e$ and $^3P^o$, respectively. In this work, we determine the bound state $^1S^e$ ($J=0, \nu=0$) and $^3P^o$ ($J=1, \nu=0$) state energies of the muonic molecular ion in Debye plasma environments. For bound state calculations, one needs to obtain the solutions of the Schrödinger equation $H\Psi = E\Psi$, where $E < 0$ following the Rayleigh-Ritz variational principle. The lowest values of the bound S and P states energies are obtained with the optimized choice of the nonlinear variational parameters following the scheme (3) as shown above. The bound 1S and 3P state energies obtained from our calculations are presented in Fig. 1, and in Table I along with the $p\mu(1S)$ threshold energies. The $p\mu(1S)$ energies are calculated by diagonalizing the Hamiltonian with the standard Slater type orbitals. From Fig. 1 and Table I, it is clear that the bound states energies increase with increasing plasma strengths and ultimately very close to the $p\mu(1S)$ threshold when the screening effect is increased further. The two systems approach the continuum near $\lambda=1.02$. ($D=0.98$) Also from Table I, it seems that our results differ by 3×10^{-13} for the S and P states as compared with the best results in the literature [7–9] for the unscreened case. For the 1S state calculations we use $N=700$ terms and for the 3P states calculations, $N=800$ terms. We have also examined convergence with the increasing number of terms in the basis expansion, and with different nonlinear parameters in the vicinity of the optimized values of the nonlinear variational parameters in the wave functions (2).

IV. RESONANCE STATES OF $pp\mu$ EMBEDDED IN DEBYE PLASMAS

Once the optimum value of the nonlinear parameters in the wave function (2) for the bound $^1S^e$ and $^3P^o$ states are obtained, we can then carry out resonance calculations for

TABLE I. The bound $^1S^e$ and $^3P^o$ states energies (in m.a.u.) of the $pp\mu$ molecular ion in plasmas for different Debye lengths along with the $p\mu(1S)$ threshold energies.

D	1S : 700 terms	3P : 800 terms	$p\mu(1S)$
∞	-0.494 386 820 248 6 -0.494 386 820 248 9 ^a	-0.468 458 436 303 04 -0.468 458 436 303 38 ^a	-0.449 393 964 391 0
100	-0.484 459 898 269 7	-0.458 533 814 176 6	-0.439 476 800 427 3
50	-0.474 677 153 911 1	-0.448 757 903 042 6	-0.429 722 941 023 7
20	-0.446 166 894 443 7	-0.420 294 763 062 7	-0.401 408 098 424 9
10	-0.401 304 651 270 3	-0.375 598 934 548 5	-0.357 198 173 531 3
8	-0.380 053 630 148 2	-0.354 472 467 681 9	-0.336 407 781 840 0
6	-0.346 294 636 941 8	-0.320 982 657 529 7	-0.303 588 302 718 7
4	-0.284 644 528 236 4	-0.260 101 051 184 7	-0.244 352 635 123 7
3	-0.230 267 151 647 6	-0.206 793 071 528	-0.192 946 216 788 7
2.5	-0.191 628 586 262 8	-0.169 220 188 998	-0.156 991 245 827 3
2.0	-0.141 220 404 435 6	-0.120 750 832 04	-0.111 002 308 076 7
1.5	-0.075 713 948 758	-0.059 372 294 9	-0.053 625 369 945 2
1.2	-0.031 226 122 7	-0.020 192 25	-0.017 874 385 443 5
1.1	-0.017 442 512 9	-0.009 269	-0.008 150 899 921
1.0	-0.005 998 2	-0.001 71	-0.001 520 383 8
0.98	-0.004 190 8		-0.000 761 4

^aReferences [7–9].

such angular momentum states of the $pp\mu$ molecular ion using the stabilization method [25–27]. One can diagonalize the atomic Hamiltonian to calculate the energy levels $E(\omega)$ by varying the scaling factor ω in Eq. (2). The scaling factor ω is considered as the reciprocal range of a “soft” wall [14,21,26,27]. In the stabilization method, the energy levels are then plotted to obtain a stabilization diagram [see Fig. 2(a)] that provides the behavior of the energy spectrum. A flat plateau in the energy diagram can be interpreted as a resonance, and from which the resonance position and width can be deduced. In this work, it is sufficient to vary ω in the range 0.3–1.0 with mesh size 0.001.

To extract the resonance energy E_r and the resonance width Γ , we calculate the density of resonance states for a single energy level using the formula

$$\rho_n(E) = \left| \frac{E_n(\omega_{i+1}) - E_n(\omega_{i-1})}{\omega_{i+1} - \omega_{i-1}} \right|_{E_n(\omega_i)=E}^{-1}, \quad (4)$$

where the index i is the i th value for ω and the index n is for the n th resonance. After calculating the density of resonance states $\rho_n(E)$ using formula (4), we fit it to the following Lorentzian form that yields resonance energy E_r and a total width Γ , with

$$\rho_n(E) = y_0 + \frac{A}{\pi} \frac{(\Gamma/2)}{(E - E_r)^2 + (\Gamma/2)^2}, \quad (5)$$

where y_0 is the baseline offset, A is the total area under the curve, E_r is the center of the peak, and Γ denotes the full width of the peak of the curve at half height.

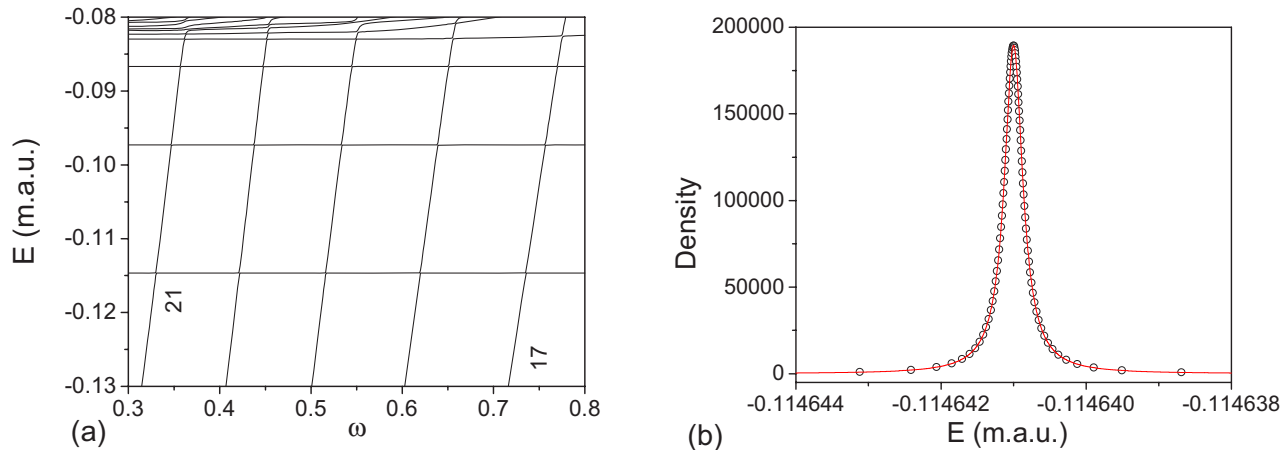


FIG. 2. (Color online) (a) Stabilization plots and (b) the best fitting (solid line) of the calculated density of states (circles) for the lowest $^1S^e$ resonance of the $pp\mu$ molecular ion immersed in plasmas for $D=30$.

TABLE II. The ${}^1S^e$ resonance energies, E_r (m.a.u.), of the $pp\mu$ molecular ion in plasmas for different Debye lengths along with the $p\mu(2S)$ threshold energies.

D	${}^1S^e(1)$	${}^1S^e(2)$	${}^1S^e(3)$	${}^1S^e(4)$	$p\mu(2S)$
∞	-0.146 404 68 -0.146 404 68 ^a	-0.128 885 488 -0.128 885 489 ^a	-0.118 028 793 -0.118 028 794 ^a	-0.113 949 7 -0.113 949 7 ^a	-0.112 348 491 1 -0.112 348 490 69 ^a
100	-0.136 539 60	-0.119 028 59	-0.108 184 07	-0.104 121 9	-0.102 673 998 9
50	-0.126 955 93	-0.109 483 61	-0.098 694 93	-0.094 716 5	-0.093 620 180 8
30	-0.114 641 00	-0.097 294 56	-0.086 680 20	-0.082 967 8	-0.082 445 090 6
20	-0.100 029 63	-0.082 991 03	-0.072 787 34	-0.069 78	-0.069 806 438 0
15	-0.086 322 75	-0.069 781 14	-0.060 236 6		-0.058 525 442 3
10	-0.061 720 33	-0.046 784 44	-0.039 679		-0.039 618 578 8
8	-0.045 795 89	-0.032 639 16			-0.028 301 237 7
6	-0.024 251 33	-0.015 302 5			-0.014 202 375 1
5	-0.011 789 88	-0.006 886			-0.006 699 580
4	-0.001 69				-0.000 835

^aReference [7].

Once the position of the resonances are identified from the flat regions of the stabilization plots, then in the next step of the stabilization method one needs to calculate the density of resonance states using formula (4) in the stabilized region of each energy level. The density is then fitted to the Lorentzian form (5) to obtain the resonance parameters (E_r, Γ). The fit that leads to the least chi-square and with the square of the correlation coefficient closer to 1 is considered as the best fit, the resonance parameters (E_r, Γ) are considered as the best value for that particular state. In Fig. 2(b) we present the best fit for the lowest ${}^1S^e$ resonance of the $pp\mu$ molecular ion immersed in plasmas for $D=30$ corresponding to the 21st energy level in the stabilization plot Fig. 2(a). In a similar way, we have extracted the resonance energies and widths for various Debye lengths. We present the calculated ${}^1S^e$ and ${}^3P^o$ resonance energies in Tables II and III, respectively, and the corresponding resonance widths in Table IV. We also show our calculated resonance parameters in Figs. 3 and 4. In Tables II and III and Figs. 3(a) and 4(a), our calculated $p\mu(2S)$ threshold energies are also presented.

The results indicate that the resonance energies of the $pp\mu$ molecular ion increase with increasing plasma strength, but the resonance widths, for the most part, decrease with increasing plasma strengths. For the ${}^1S^e(1)$ resonance state, we have observed that the resonance width increases somewhat when λ is first increased, but the width starts to decrease when λ is increased further. We have found four resonances below the $p\mu(2S)$ threshold supported by the Born-Oppenheimer $3d\sigma_g$ curve for each of the $J=0$ and $J=1$ states with $\nu=0, 1, 2,$ and 3 , respectively. We have obtained the widths for the lowest three resonances for the $J=0$ and $J=1$ states. The resonance widths corresponding to the fourth resonances are too narrow and we prefer not to report them here. It is evident from Tables II and IV that our calculated resonance parameters in the unscreened case are comparable with the reported results [4–6]. In Table V, we have made the comparison by converting the resonance energies in electron volts measured from the $p\mu$ ground state energy threshold. The resonance width is related to lifetime in picoseconds (10^{-12} s) using the standard relation $\Gamma(\text{in eV}) \times \tau(\text{in s}) = \hbar$,

TABLE III. The ${}^3P^o$ resonance energies, E_r (m.a.u.), of the $pp\mu$ molecular ion in plasmas for different Debye lengths along with the $p\mu(2S)$ threshold energies.

D	${}^3P^o(1)$	${}^3P^o(2)$	${}^3P^o(3)$	${}^3P^o(4)$	$p\mu(2S)$
∞	-0.144 601 123	-0.127 604 837	-0.117 294 86	-0.113 691	-0.112 348 491 1
100	-0.134 736 445	-0.117 748 627	-0.107 451 41	-0.103 865	-0.102 673 998 9
50	-0.125 154 555	-0.108 206 563	-0.097 967 74	-0.094 468	-0.093 620 180 8
30	-0.112 845 342	-0.096 026 442	-0.085 969 37	-0.082 74	-0.082 445 090 6
20	-0.098 248 047	-0.081 743 916	-0.072 114 79	-0.069 6	-0.069 806 438 0
15	-0.084 564 279	-0.068 567 195	-0.059 631 92		-0.058 525 442 3
10	-0.060 038 408	-0.045 678 145	-0.039 4		-0.039 618 578 8
8	-0.044 200 143	-0.031 660 611			-0.028 301 237 7
6	-0.022 862 963	-0.014 692 48			-0.014 202 375 1
5	-0.010 650 247				-0.006 699 580
4					-0.000 835

TABLE IV. The $^1S^e$ and $^3P^o$ resonance widths, Γ (m.a.u.), corresponding to the resonance energies in Tables II and III, respectively, of the $pp\mu$ molecular ion in plasmas for different Debye lengths.

D	$^1S^e(1)$ (10^{-7})	$^1S^e(2)$ (10^{-7})	$^1S^e(3)$ (10^{-7})	$^3P^o(1)$ (10^{-7})	$^3P^o(2)$ (10^{-7})	$^3P^o(3)$ (10^{-7})
∞	3.073	5.36	3.94	2.14	3.33	2.28
	3.026 ^a	5.25 ^a	4.124 ^a	2.16 ^b	3.47 ^b	2.48 ^b
100	3.075	5.36	3.93	2.13	3.32	2.27
50	3.078	5.35	3.89	2.12	3.29	2.22
30	3.073	5.28	3.76	2.08	3.21	2.07
20	3.026	5.08	3.49	2.00	3.01	1.74
15	2.917	4.73		1.86	2.71	
10	2.500	3.62		1.48	1.91	
8	2.033	2.55		1.09	1.20	
6	1.130	0.759				
5	0.485					

^aReference [7].

^bReference [5].

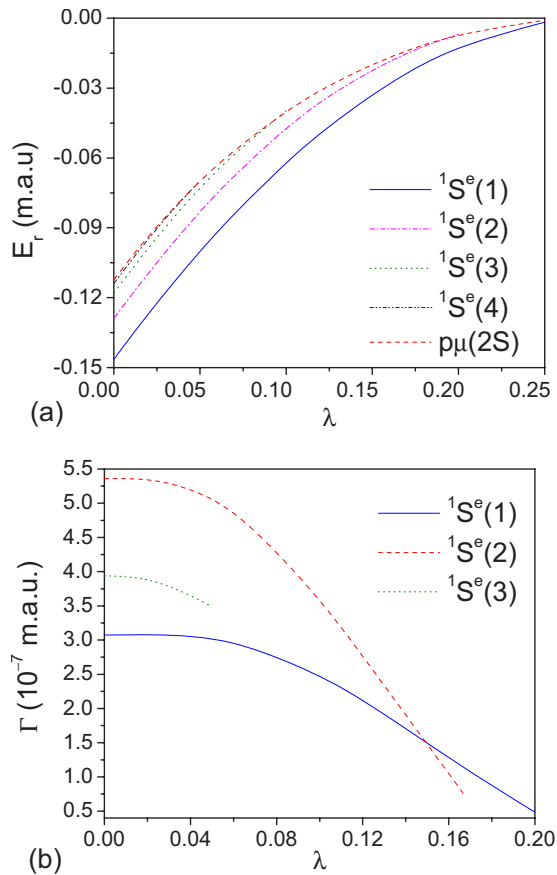


FIG. 3. (Color online) (a) $^1S^e$ resonance energies and (b) the corresponding resonance widths of the $pp\mu$ molecular ion for different screening parameters.

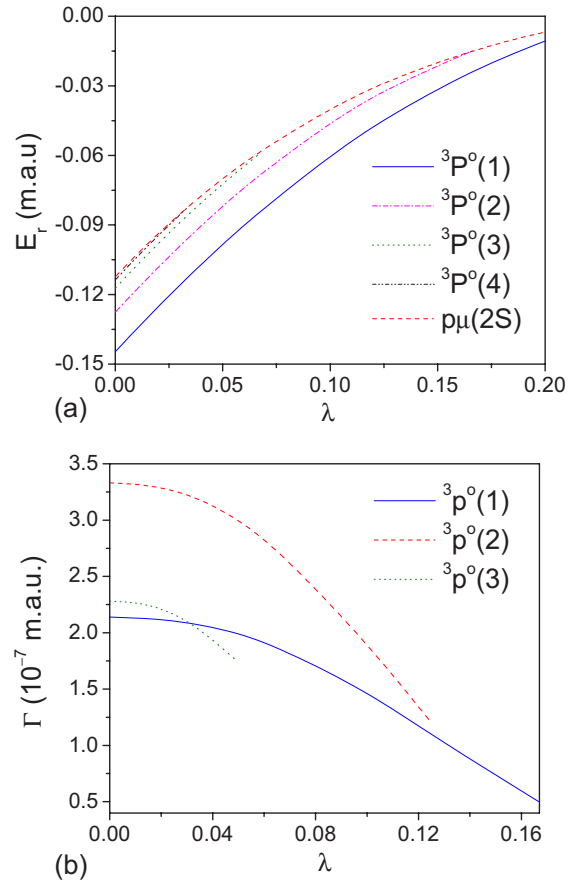


FIG. 4. (Color online) (a) $^3P^o$ resonance energies and (b) the corresponding resonance widths of the $pp\mu$ molecular ion for different screening parameters.

where τ denotes the lifetime of the autoionization process and $\hbar = 6.58211 \times 10^{-16}$ eV s. The autoionization rate is related to the inverse of the autoionization lifetime. The muon atomic unit (m.a.u.) is used in Figs. 1–4 and Tables I–IV. We employ 600 and 800 term basis functions (2) for S and P resonance states, respectively. We have observed quite reasonable convergence in our calculations with an increasing number of terms used in the basis sets.

Next we discuss the relevance of our present investigation in light of the recent experimental activities on muonic atoms. Since the magnitude of the cross sections in the direct Coulombic deexcitation process is too small at the $n=2$ level to explain the existence of high energy $p\mu(1S)$ atoms, a feasible source to investigate the high energy $p\mu(1S)$ atoms is the Coulomb decay of plasma-embedded $pp\mu$ molecular ions. An atom or molecule immersed in plasma experiences various perturbations from the plasmas leading to a definitive distribution of atom or molecule. Due to such perturbation the atomic or molecular states turn out to be *mixed* substantially different from the *pure* unperturbed atomic or molecular states. The muon is strongly localized to the proton and weakly perturbed by this heavy particle. The PSI experiment indicates that a Coulombic deexcitation rate for $p\mu(2S)$ atoms in liquid hydrogen density (LHD) of the order of $4 \times 10^{11} \text{ s}^{-1}$ would be required to explain the results of the

TABLE V. Comparison of the resonance parameters of the $pp\mu$ molecular ion in the unscreened case with the available results. Resonance energies (in eV) are measured from the ($p\mu$) ground state threshold. Γ is the autoionization rate in $(\text{ps})^{-1}$.

States	Resonance parameters	Present work	Hilico <i>et al.</i> [5]	Lindroth <i>et al.</i> [6]	Kilic <i>et al.</i> [7]
$^1S^e(1)$	$E_r(\text{eV})$	191.615 46	191.615	191.616	191.615 470
	$\Gamma(\text{ps})^{-1}$	2.63	2.59	2.59	2.587
$^1S^e(2)$	$E_r(\text{eV})$	93.044 59	93.045	93.046	93.044 604
	$\Gamma(\text{ps})^{-1}$	4.58	4.49	4.49	4.487
$^1S^e(3)$	$E_r(\text{eV})$	31.959 94	31.960	31.960	31.959 948
	$\Gamma(\text{ps})^{-1}$	3.37	3.52	3.40	3.526
$^1S^e(4)$	$E_r(\text{eV})$	9.009 12	9.009	9.009	9.009 143
$^3P^o(1)$	$E_r(\text{eV})$	181.467 84	181.468	181.468	
	$\Gamma(\text{ps})^{-1}$	1.83	1.85	2.14	
$^3P^o(2)$	$E_r(\text{eV})$	85.839 1	85.839	85.839	
	$\Gamma(\text{ps})^{-1}$	2.85	2.97	3.53	
$^3P^o(3)$	$E_r(\text{eV})$	27.830 5	27.831	27.831	
	$\Gamma(\text{ps})^{-1}$	1.95	2.12	2.46	
$^3P^o(4)$	$E_r(\text{eV})$	7.554	7.558	7.558	

experiments [1,2]. The value of the direct Coulombic deexcitation rate obtained by extrapolation from higher n is however of the order of 10^7 – 10^8 s^{-1} [6,29]. A theoretical estimate of the molecular formation rate is reported as 5×10^{10} s^{-1} at the $n=3$ level which is 10 times lower than the quenching rate of $p\mu(2S)$ at LHD [4]. In order to obtain a more precise estimate on the quenching rate, and to detect the improved path in the muon catalyzed fusion cycle, an investigation on the shift of the molecular energy levels and the Coulomb decay seem important. From the perturbation theory, it is well known that all the isolated energy levels displaced upwards and eventually at the continuum due to screening. In general, by writing the screened Coulomb potential as

$$-\frac{Z}{r} \exp(-r/D) \approx -\frac{Z}{r} + \frac{Z}{D} - \frac{Zr}{2D^2} + \dots, \quad (6)$$

with Z denoting the nuclear charge, one can observe that the first order correction upshifts all bound levels equally but does not change the wave function [24]. The effective perturbation potential in the lowest order for the localized two particle interaction is given by $-Zr/2D^2$. Furthermore, the screened Coulomb (Yukawa-type) potentials obtained from the Debye concept of plasma modeling is a good approximation for hot-dense and low-density warm plasmas. This potential is widely used in plasma modeling to describe the shielding effects between two charged particles due to the thermal ionization in plasmas. The importance of the Debye screening on atomic and molecular ions has been highlighted in the earlier investigations ([10–22] and references therein). The validity of the Debye screening for the proposed system

is dependent on the experimental support of generating the plasma density and its temperature. With recent developments on the laser plasmas produced in the laser fusion in the laboratories, accurate atomic data for various plasma conditions are useful for plasma diagnostic purposes.

V. SUMMARY AND CONCLUSIONS

In this work, we have made a first investigation on the bound states and resonance states of $pp\mu$ molecular ion immersed in weakly coupled hot plasmas. The plasmas effect has been taken care of in the framework of the Debye shielding approach of plasma modeling that is suitable for low-density high-temperature plasmas. The bound state energies of the $^1S^e$ and $^3P^o$ states for the molecular $pp\mu$ ion in the lowest rovibronic states and the $1S$ and $2S$ state threshold energies of the $p\mu$ atom in plasmas for various Debye lengths are calculated. We have obtained four resonances for each of the $^1S^e$ and $^3P^o$ states below the $p\mu(2S)$ threshold. The stabilization method is used to extract resonance parameters for the $pp\mu$ molecular ion. This method needs only bound-state type basis functions to calculate resonances for few-body atomic and molecular systems. With recent experimental advancement in studies of muonic atoms, we hope our findings will provide new insight and play an important role in the future for research communities such as muon physics, plasma physics, and atomic and molecular physics.

ACKNOWLEDGMENT

The work is supported by the National Science Council of R.O.C.

- [1] R. Pohl, H. Daniel, F. J. Hartmann, P. Hauser, F. Kottmann, V. E. Markushin, M. Mühlbauer, C. Petitjean, W. Schott, D. Taqqu, and P. Wojciechowski-Grosshauser, *Phys. Rev. Lett.* **97**, 193402 (2006).
- [2] R. Pohl, H. Daniel, F. J. Hartmann, P. Hauser, Y. W. Liu, F. Kottmann, C. Maierl, V. E. Markushin, M. Mühlbauer, C. Petitjean, W. Schott, and D. Taqqu, *Hyperfine Interact.* **138**, 35 (2001).
- [3] F. Kottmann *et al.*, *Hyperfine Interact.*, **138**, 55 (2001).
- [4] J. Wallenius, S. Jonsell, Y. Kino, and P. Froelich, *Hyperfine Interact.* **138**, 285 (2001).
- [5] L. Hilico, N. Billy, B. Gremaud, and D. Delande, in *Proceedings of the Workshop on Molecular Effects in the Exotic Hydrogen Cascade*, edited by R. Pohl (PSI, Villigen, 2001).
- [6] E. Lindroth, J. Wallenius, and S. Jonsell, *Phys. Rev. A* **68**, 032502 (2003); **69**, 059903(E) (2004).
- [7] S. Kilic, J.-P. Karr, and L. Hilico, *Phys. Rev. A* **70**, 042506 (2004).
- [8] A. M. Frolov, *Phys. Rev. E* **64**, 036704 (2001).
- [9] D. H. Bailey and A. M. Frolov, *J. Phys. B* **35**, 4287 (2002).
- [10] S.-T. Dai, A. Solovyova, and P. Winkler, *Phys. Rev. E* **64**, 016408 (2001).
- [11] A. N. Sil and P. K. Mukherjee, *Int. J. Quantum Chem.* **102**, 1061 (2005).
- [12] H. Okutsu, T. Sako, K. Yamanouchi, and G. H. F. Diercksen, *J. Phys. B* **38**, 917 (2005).
- [13] S. Kar, Y. K. Ho, *Int. J. Quantum Chem.* **106**, 814 (2006); **107**, 353 (2007).
- [14] S. Kar and Y. K. Ho, *Phys. Rev. A* **72**, 010703 (R) (2005); *Few-Body Syst.* **40**, 13 (2006). *J. Phys. B* **40**, 2403 (2007).
- [15] S. Chakraborty and Y. K. Ho, *Chem. Phys. Lett.* **438**, 99 (2007).
- [16] L. Bertini, M. Mella, D. Bressanini, and G. Morosi, *Phys. Rev. A* **69**, 042504 (2004).
- [17] J.-M. Richard, *Few-Body Syst.* **38**, 79 (2006).
- [18] P. K. Mukherjee, S. Fritzsche, and B. Fricke, *Phys. Lett. A* **360**, 287 (2006).
- [19] S. Kar and Y. K. Ho, *Phys. Lett. A* (to be published).
- [20] B. Shaha, P. K. Mukherjee, and G. H. F. Diercksen, *Astron. Astrophys.* **396**, 337 (2002).
- [21] S. Kar and Y. K. Ho, *New J. Phys.* **7**, 141 (2005).
- [22] L. Zhang and P. Winkler, *Chem. Phys.* **329**, 338 (2006).
- [23] S. Ichimaru, *Plasma Physics* (Benjamin/Cummings Publishing Company, Inc., Menlo Park, CA, 1986).
- [24] H. R. Griem, in *Principles of Plasma Spectroscopy*, Cambridge Monograph in Plasma Physics Vol. 2, (Cambridge University Press, Cambridge, UK, 2005).
- [25] V. A. Mandelshtam, T. R. Ravuri, and H. S. Taylor, *Phys. Rev. Lett.* **70**, 1932 (1993).
- [26] S. S. Tan and Y. K. Ho, *Chin. J. Phys. (Taipei)* **35**, 701 (1997).
- [27] S. Kar and Y. K. Ho, *J. Phys. B* **37**, 3177 (2004).
- [28] A. M. Frolov, V. H. Smith, Jr., and D. M. Bishop, *Phys. Rev. A* **49**, 1686 (1994).
- [29] A. V. Kravtsov, A. I. Mikhailov, L. I. Ponomarev, and E. A. Solovyov, *Hyperfine Interact.* **138**, 99 (2001).